Influence of Geometry of Joint on Strength of Ceramic Composite Joint †

SERIZAWA Hisashi*, LEWINSOHN Charles A. ** and MURAKAWA Hidekazu ***

Abstract

In order to examine the influence of the geometry of the joint on the strength of ceramic joints, the interface element was proposed as one of the simple models which represent the mechanism of failure in an explicit manner. It was applied to the analysis of the fracture strength of SiC/SiC composite specimen joined by ARCJoinT™, and the effect of the scarf angle on the joint strength was studied by changing the scarf angle between the composite and the joint. It was clearly shown that the joint strength was governed both by the surface energy and the bonding strength. Moreover, it was found that the strength was affected by the order of the singularity in the stress field. Thus, the proposed method was considered to have a great potential as a tool to study the failure problems of various structures.

KEY WORDS: (Interface Element) (Finite Element Method) (SiC/SiC Composite) (Surface Energy) (Joint) (Fracture)

1. Introduction

Silicon carbide based fiber reinforced silicon carbide composites (SiC/SiC composites) are promising candidate materials for high heat flux components because of their high temperature properties, chemical stability and good oxidation and corrosion resistance[1-5]. For fabricating large or complex shaped parts of SiC/SiC composites, the technique of joining between simple geometrical shapes is considered to be an economical and useful method. Joints must retain their structural integrity at high temperatures and must have mechanical strength and environmental stability comparable to the bulk materials. As a result of R & D efforts, an affordable, robust ceramic joining technology (ARCJoinT™) has been developed as one of the most suitable methods for joining SiC/SiC composites among various types of joining between ceramic composites[6].

To establish useful design databases, the mechanical properties of joints must be accurately measured and quantitatively characterized, where the tensile strength of joints is the most basic and important mechanical property. Bending tests have been used widely to measure the tensile strength of SiC/SiC composites at high temperatures[7,8], but the tensile test is preferable method since a pure tensile stress can be applied to the entire specimen. Recently, a new technique of tensile testing using a small specimen of SiC/SiC composite has been proposed[9].

The strength of the bonded joint is largely influenced by the geometry of the joint. In order to study this influence, the level of stress and the order of the singularity in the stress field are commonly employed for the relative evaluation of strength. Although detailed information on the stress field is provided, little information on the criteria of the fracture is obtained from these types of study. This comes from the fact that, the physics of failure itself is not explicitly modeled in these analyses. The interface element, which directly models the formation of the surface may have potential capability, not only to give insight into the criteria of the fracture, but also to make the quantitative prediction of strength itself. So, in this research, the effect of the joint shape on the stress singularity and the strength was studied for the tensile test of the SiC/SiC composite joint by using the interface element.

2. Interface Potential

Essentially, the interface element is the distributed nonlinear spring existing between surfaces forming the

† Received on May 31, 2002
* Research Associate
** Ceramatec, Inc.
*** Professor

Transactions of JWRI is published by Joining and Welding Research Institute of Osaka University, Ibaraki, Osaka 567-0047, Japan

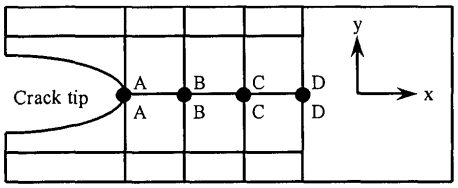

(a) Before Crack Propagation

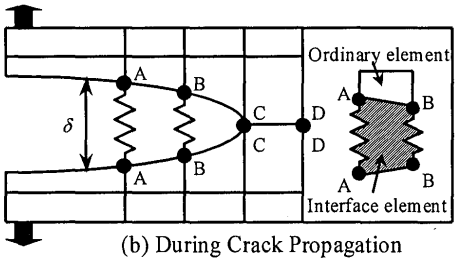

(b) During Crack Propagation

Fig.1 Representation of crack growth using interface element.

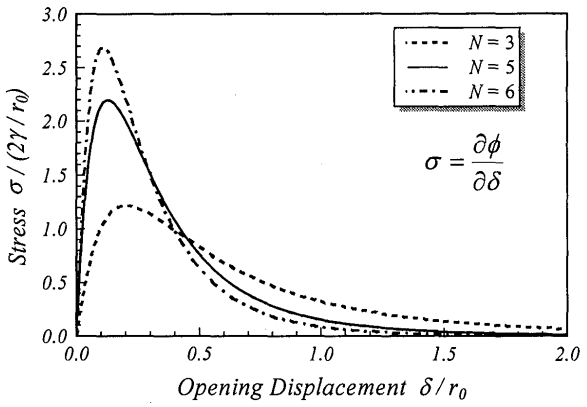

Fig.2 Relation between crack opening displacement and bonding stress.

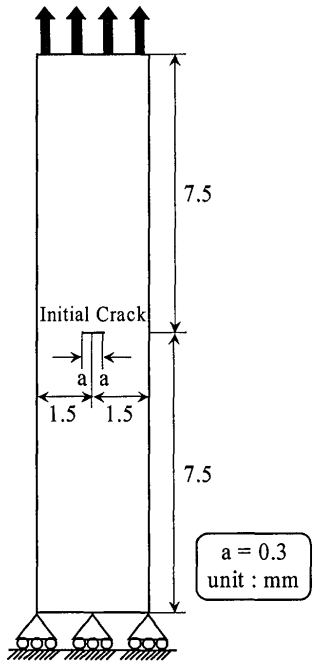

Fig.3(a) Plate with center crack.

interface or the potential crack surfaces as shown by **Fig.1**. The relation between the opening of the interface δ and the bonding stress σ is shown in **Fig.2**. When the opening δ is small, the bonding between two surfaces is maintained. As the opening δ increases, the bonding stress σ increases till it becomes the maximum value σ_{cr} at the opening δ_{cr}. With further increase of δ, the bonding strength is rapidly lost and the surfaces are completely separated. Such interaction between the surfaces can be described by the interface potential. There are rather wide choices for this potential. The authors employed the Lennard-Jones type potential because it explicitly involves the surface energy γ which is necessary to form new surfaces. Thus, the surface potential per unit surface area ϕ can be defined by the following equation.

$$\phi(\delta) = 2\gamma \cdot \left\{ \left(\frac{r_0}{r_0 + \delta} \right)^{2N} - 2 \cdot \left(\frac{r_0}{r_0 + \delta} \right)^{N} \right\}, \qquad (1)$$

where, constants γ, r_0, and N are the surface energy per unit area, the scale parameter and the shape parameter of the potential function. The derivative of ϕ with respect to the opening displacement δ gives the bonding stress σ acting on the interface,

$$\sigma = \frac{\partial \phi}{\partial \delta} = \frac{4\gamma N}{r_0} \cdot \left\{ \left(\frac{r_0}{r_0 + \delta} \right)^{N+1} - \left(\frac{r_0}{r_0 + \delta} \right)^{2N+1} \right\} \qquad (2)$$

As is seen from the above equation, the bonding stress σ is proportional to the surface energy γ and inversely proportional to the scale parameter r_0.

By arranging such interface elements along the crack propagation path as shown in Fig. 1, the growth of the crack under the applied load can be analyzed in a natural manner. In this case, the criteria for crack growth based on the comparison between the driving force and the resistance as in the conventional methods are not necessary.

3. Influence of Parameters

Among three parameters involved in the interface energy function, only the surface potential γ has a clear physical meaning. While those of the scale parameter r_0 and the shape parameter N are not very clear. To clarify the influence of the scale parameter r_0 on the numerical results of the failure problem, the brittle fracture of a SiC/SiC composite plate with a center crack under tensile load was analyzed assuming linear elastic behavior in two dimensional plain stress. Young's modulus and Poisson's ratio were set to 300 GPa and 0.3, respectively. **Figure 3(a)** shows the model where the plate was loaded through the vertical displacement given on one end of the plate. The value of the surface energy γ of the SiC/SiC composite was assumed to be 30 N/m

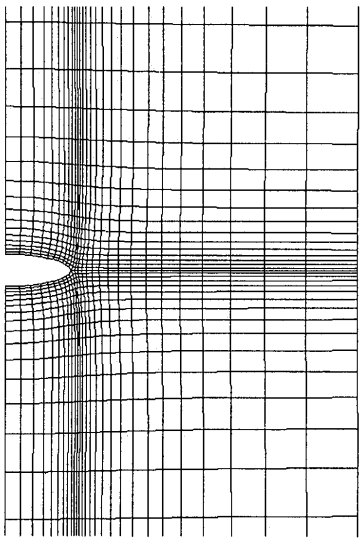

Fig.3(b) Mesh division near crack tip superposed on deformation.

according to a result of the compact tension test[10] and the shape parameter N was set to 4 in relation with our previous researches[11]. The value of the scale parameter was changed from 1.0 x 10^{-4} to 100 μm. One half of the plate was the model and divided into 27 x 50 meshes, where the mesh division near the crack tip was set to fine as shown in **Fig.3(b)**.

Figure 4(a) shows the load-displacement curves in cases of r_0 = 0.3, 0.5, 0.7, 1.0, 3.0 μm and the relations between the opening displacement at the crack tip and the applied displacement are also as shown in **Fig.4(b)**. When the scale parameter was large, such as the case with r_0 = 3.0 μm, stable crack growth was observed just after the maximum load and the computation stops due to the loss of stability. On the other hand, when the scale parameter was small, the instability occurred suddenly without clear increase of the opening displacement or the drop of load. The load at the loss of stability was defined as the point of fracture. The influence of the scale parameter is summarized in **Fig.5** with logarithmic scale. For comparison, the fracture load computed using the analytical formula is shown in the figure. As is clearly seen from the figure, the curve could be divided into three parts with respect to the size of the scale parameter r_0. When r_0 was between 0.05 and 0.5 μm, the fracture load was almost independent of the scale parameter and the value was almost the same as the analytical result. When the scale parameter was smaller or larger than this range, the slope of the curve became -1. This could be explained in the following way. The middle part corresponded to the brittle fracture of the plate with crack growth. Thus, the critical load was determined only by the surface energy γ and independent of r_0. According to Eq.(2), the bonding strength and the rigidity of the interface became small with the increase

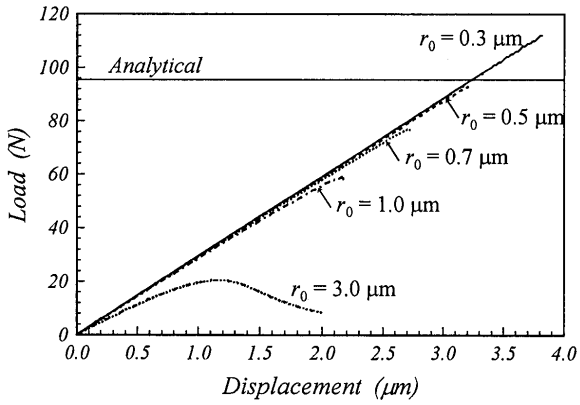

Fig.4(a) Load-displacement curves of plate with center crack.

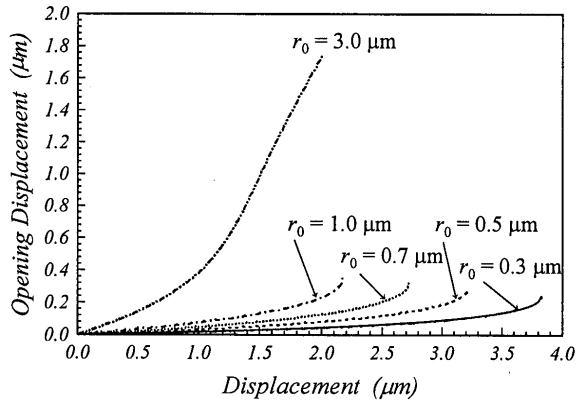

Fig.4(b) Applied displacement-crack tip opening in plate with center crack.

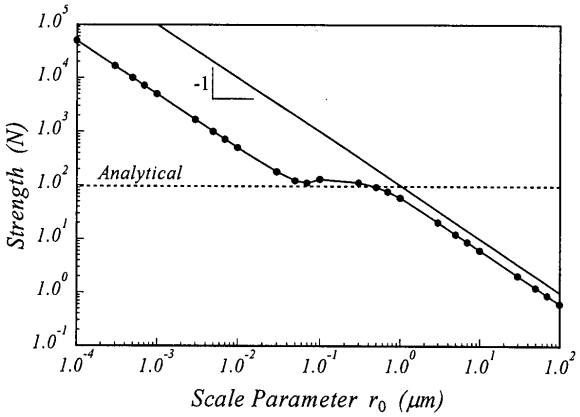

Fig.5 Effect of scale parameter on predicted strength of plate with center crack.

of the scale parameter. Therefore, the plate broke in the separation mode without significant deformation of the plate or crack growth when the scale parameter was large. On the other hand, bonding strength became larger than the stress induced at the crack tip in FEM model, when the scale parameter was small. In this case, the instability was not governed by the surface energy γ but by the bonding strength σ_{cr}. These computed results clearly show that the failure mode and the stability limit depend on the combination of the deformability of the plate and the mechanical properties of the interface.

On the other hand, from our previous studies about the peeling of two bonded elastic strips, the scale parameter r_0, the shape parameter N and the mesh division had no influence on the peeling process and the process was mainly governed by the surface energy γ[12,13].

4. Strength of Ceramic Joint

4.1 Model for analysis

As an example of a ceramic joint, a SiC/SiC composite specimen jointed by ARCJoinT^{TM} as shown in **Fig.6** was analyzed. The length, the width and the thickness were 15 mm, 3mm and 1 mm, respectively according to the proposed tensile test[9]. The thickness of the joint was set to 100 μm, for a typical example of ARCJoinT^{TM} [6,14]. Young's moduli and Poisson's rations of SiC/SiC composite and the joint were assumed to be 300 GPa, 393 GPa, 0.3 and 0.19, respectively[15].

In order to examine the effect of scarf angle on the joint strength, the mechanical properties of the interface element need to be defined for both the opening and the shear modes since the mode of the failure is mixed. Though the interaction between the two modes is expected, only the case when they are independent was reported as the preliminary analysis. Their interaction will be reported in the future. According to this assumption, the interface potential ϕ could be defined as a sum of those for the opening mode ϕ_n and the shear mode ϕ_t as in the following equations.

$$\phi(\delta_n,\delta_t) \equiv \phi_n(\delta_n)+\phi_t(\delta_t) \tag{3}$$

$$\phi_n(\delta_n) = 2\gamma_n \cdot \left\{ \left(\frac{r_{0n}}{r_{0n}+\delta_n} \right)^{2N} - 2 \cdot \left(\frac{r_{0n}}{r_{0n}+\delta_n} \right)^{N} \right\} \tag{4}$$

$$\phi_t(\delta_t) = 2\gamma_t \cdot \left\{ \left(\frac{r_{0t}}{r_{0t}+|\delta_t|} \right)^{2N} - 2 \cdot \left(\frac{r_{0t}}{r_{0t}+|\delta_t|} \right)^{N} \right\} \tag{5}$$

Where, δ_n and δ_t were the opening and the shear deformations of the interface. Due to the symmetry of the shear deformation, the interface potential for the shear mode ϕ_t was assumed as a symmetric function of the shear deformation δ_t as shown in **Fig.7**.

Although the tensile strength of the composite joint was experimentally found to be different from the shear strength[6,14], the surface energies γ_n, γ_t were assumed to be 3 N/m equally according to the fracture energy of a porous ceramic layer[16]. In order to examine the influence of scarf angle θ on the joint strength, the interface elements were arranged along the lower interface between SiC/SiC composite and the joint.

4.2 Effect of scarf angle on joint strength

In order to examine the influence of the scarf angle

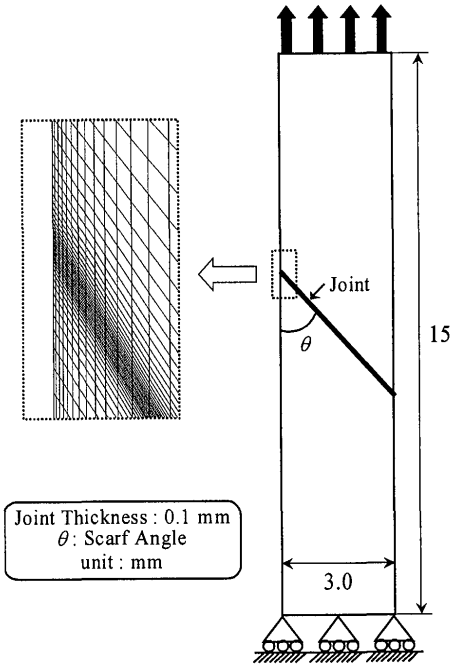

Fig.6 Model and mesh division of ceramic joint.

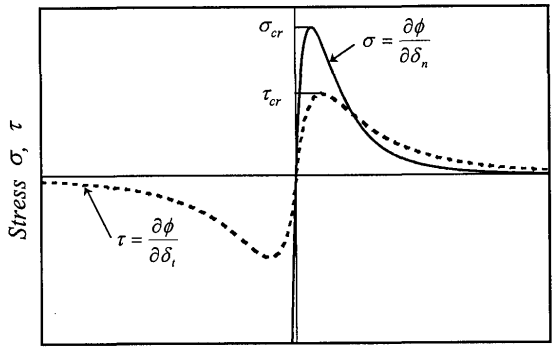

Fig.7 Displacement-stress relation at interface for opening and shear modes.

on the joint strength, the strength was calculated through the serial computations where the scale parameters r_{0n}, r_{0t} were equally varied from 1.0 x 10^{-4} to 100 μm and the scarf angle θ was changed from 30 to 150 degree. As expected from the assumption of the interface potential in Eq.(4), the mode of the failure changed at 45 or 135 degree with increasing the scarf angle. The effects of the scale parameters and the scarf angle on the joint strength are summarized in **Fig.8(a)**. As opposed to the case of center cracked plate discussed in the preceding chapter, the horizontal part was not observed in the composite joint. This means that the joint strength was not determined by the surface energies γ_n, γ_t alone. It was governed by both the surface energies and the bonding strength σ_{cr}. **Figure 8(b)** shows the relations to the scale parameter between the scale parameters and the ratio of the opening or shear displacement at the edge of the interface in the failure. As mentioned in the previous

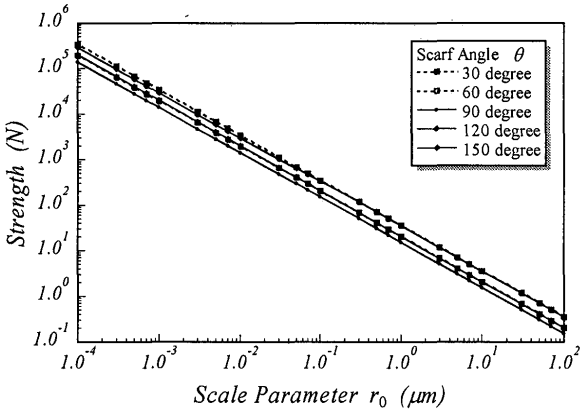

Fig.8(a) Effect of scale parameter on predicted strength of ceramic joint.

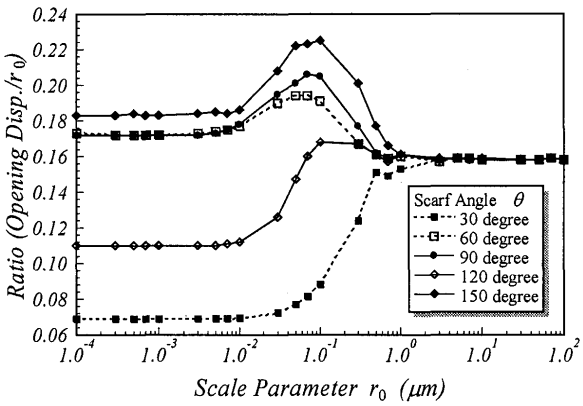

Fig.8(b) Influence of scale parameter on ratio of opening or shear displacement.

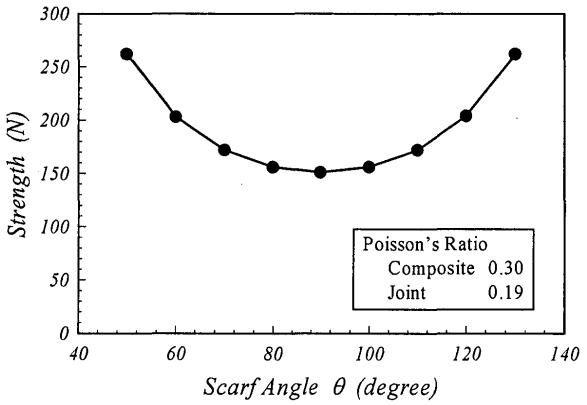

Fig.9(a) Effect of scarf angle on predicted strength of ceramic joint.

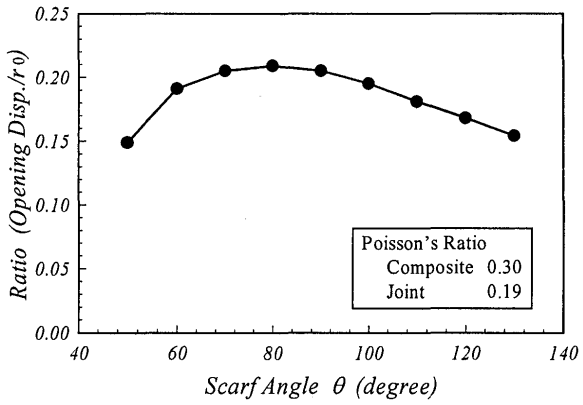

Fig.9(b) Influence of scarf angle on ratio of opening displacement.

section, when the scale parameter r_0 was small or large the strength was dependent on the stress, which means that the opening displacement at the interface in the failure was also dependent on the scale parameter. So, though the slope of the curves in Fig.8(a) was almost constant, it was found that the influence of the scale parameters on the joint strength could be divided into three parts from Fig.8(b) the same as the case of center cracked plate. Namely, the joint strength was strongly influenced by the bonding strength in the range larger than 1 μm or smaller than 0.01 μm. While, the surface energy became influential in the other area.

In order to closely study the influence of the scarf angle, the relation between the joint strength and the scarf angle was summarized in **Fig.9(a)** where the scale parameters was 0.1 μm since the joint strength was considered to be affected by both the bonding strength and the surface energy. **Figure 9(b)** shows the effect of scale parameters on the ratio of the opening displacement to the scale parameter. The joint strength became small when the scarf angle was around 90 degrees. On the other hand, the ratio shows an almost opposite dependency. Since the strength of joint materials was largely affected by the stress singularity cased by the mismatch of the mechanical properties, the influence of the scarf angle on the order of the singularity was calculated. As a result, by using Dunders's parameter[17,18], the order of the singularity became the maximum at the scarf angle $\theta = 94$ degree and the minimum at $\theta = \pm 42$ degree. Though the joint strength is not determined by the order of the singularity in the stress field, this result suggested a strong relation between the order of the singularity and the joint strength.

4.3 Effect of stress singularity

Since the order of the stress singularity is affected by the mechanical properties of both base and joint materials. In the case that Young's moduli and Poisson's ratio of SiC/SiC composite and the joint were 300 GPa, 393 GPa, 0.19 and 0.19, respectively, the scarf angle at the minimum singularity changed to be ±64 degree, though that at the maximum singularity was almost the same. So the effects of the scarf angle on the joint strength and the ratio of the opening displacement to the scale parameter were calculated under the above conditions and summarized in **Figs.10(a)** and **10(b)**. Though the order of stress singularity changed, the

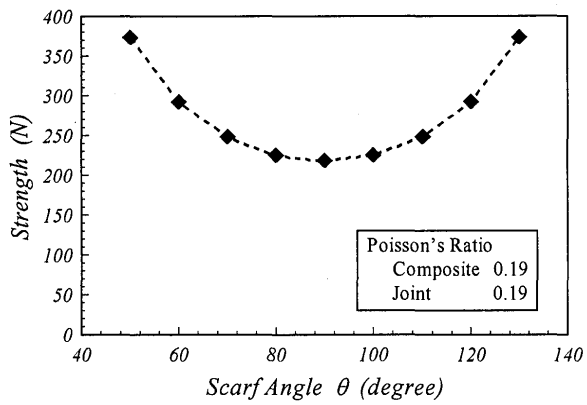

Fig.10(a) Effect of scarf angle on predicted strength of ceramic joint.

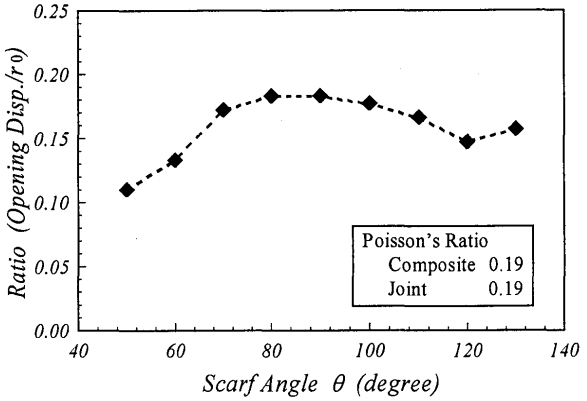

Fig.10(b) Influence of scarf angle on ratio of opening displacement.

influence of the scarf angle on the joint strength was not affected. The reason was considered to be the small difference of Young's modulus between SiC/SiC composite and the joint. The ratio of the opening displacement in failure, however, was largely affected by the change of the singularity, which means that the deformability at the joint interface was strongly dependent on the order of the singularity in the stress field.

5. Conclusions

The interface element was proposed as one of the simple models which represent the mechanism of failure in an explicit manner. It was applied to the analyses of the fracture strength of a plate with an initial crack and SiC/SiC composite specimen jointed by ARCJoinT^{TM}. The conclusions can be summarized as follows.

(1) In case of the plate with a center crack, the computed fracture load agreed fairly well with the analytical solution when the failure mode was the crack growth type, namely dependent on the surface energy of crack.

(2) In case of a ceramic composite joint, it was clearly shown that the strength was governed both by the surface energy and the bonding strength.

(3) It was found that the strength of the ceramic composite joint was affected by the order of the singularity in the stress field. Moreover, the deformability at the joint interface was considered to be strongly dependent on the stress singularity.

(4) The proposed method with the interface element was considered to have a great potential as a tool to study the failure problems of various structures.

Acknowledgements

The authors are extremely grateful to Dr. M. Singh, NASA Glenn Research Center, for valuable information. This work was supported by Core Research for Evolution Science and Technology : Advanced Material Systems for Conversion of Energy.

References

1) P. J. Lamicq, G. A. Bernhart, M. M. Dauchier and J. G. Mace, Am. Ceram. Soc. Bull., 65 [2], 336 (1986).
2) J. R. Strife, J. J. Brennan and K. M. Prewo, Ceram. Eng. Sci. Proc., 11 [7-8], 871 (1990).
3) R. H. Jones and C. H. Henager, Jr., J. Nucl. Mater., 212-215, 830 (1994).
4) R. H. Jones, C. A. Lewinsohn, G. E. Youngblood and A. Kohyama, Key Engineering Materials, 164-165, 405 (1999).
5) H. Serizawa, C. A. Lewinsohn, G. E. Youngblood, R. H. Jones, D. E. Johnston and A. Kohyama, Ceram. Eng. Sci. Proc., 20 [4], 443 (1999).
6) M. Singh, Key Engineering Materials, 164-165, 415 (1999).
7) C. H. Henager, Jr. and R. H. Jones, J. Am. Ceram. Soc., 77 [9], 2381 (1994).
8) C. A. Lewinsohn, C. H. Henager, Jr. and R. H. Jones, Ceramic Transactions, 74, 423 (1996).
9) K. Hironaka, T. Nozawa, T. Taguchi, Y. Katoh, L. L. Snead and A. Kohyama, Ceram. Eng. Sci. Proc., 23 (to be published).
10) R. K. Bordia, D. H. Roach and S. M. Salamone, Proc. 10th Int. Conf. Comp. Mater., IV, 711 (1995).
11) M. Ando, H. Serizawa and H. Murakawa, Ceram. Eng. Sci. Proc., 21 [3], 195 (2000).
12) Z. Q. Wu, H. Serizawa and H. Murakawa, Key Engineering Materials, 166, 25 (1999).
13) H. Murakawa, H. Serizawa and Z. Q. Wu, Ceram. Eng. Sci. Proc., 20 [3], 309 (1999).
14) C. A. Lewinsohn, R. H. Jones, M. Singh, T. Nozawa, M. Kotani, Y. Katoh and A. Kohyama, Ceram. Eng. Sci. Proc., 22 [4], 621 (2001).
15) H. Serizawa, C. A. Lewinsohn and H. Murakawa, Ceram. Eng. Sci. Proc., 22 [4], 635 (2001).
16) B. F. Sorensen and A. Horsewell, J. Am. Ceram. Soc., 84 [9], 2051 (2001).
17) J. Dunders, J. Appl. Mech., 36, 650 (1969).
18) J. Dunders, J. Composite Materials, 1, 310 (1967).